Hydrol. Earth Syst. Sci. Discuss., 5, 865–902, 2008
www.hydrol-earth-syst-sci-discuss.net/5/865/2008/

Hydrology and Earth System Sciences Discussions

Papers published in *Hydrology and Earth System Sciences Discussions* are under open-access review for the journal *Hydrology and Earth System Sciences*

Use of regional climate model simulations as input for hydrological models for the Hindukush–Karakorum–Himalaya region

M. Akhtar[1]**, N. Ahmad**[1]**, and M. J. Booij**[2]

[1]Institute of Geology, University of the Punjab, Lahore, Pakistan
[2]Dept. of Water Engineering and Management, Univ. of Twente, Enschede, The Netherlands

Received: 20 February 2008 – Accepted: 26 February 2008 – Published: 26 March 2008

Correspondence to: M. Akhtar (akhtarme@yahoo.com)

Published by Copernicus Publications on behalf of the European Geosciences Union.

Abstract

The most important climatological inputs required for the calibration and validation of hydrological models are temperature and precipitation that can be derived from observational records or alternatively from regional climate models (RCMs). In this paper, meteorological station observations and results of the PRECIS (Providing REgional Climate for Impact Studies) RCM driven by the outputs of reanalysis ERA-40 data and HadAM3P general circulation model (GCM) results are used as input in the hydrological model. The objective is to investigate the effect of precipitation and temperature simulated with the PRECIS RCM nested in these two data sets on discharge simulated with the HBV model for three river basins in the Hindukush-Karakorum-Himalaya (HKH) region. Three HBV model experiments are designed: HBV-Met, HBV-ERA and HBV-Had where HBV is driven by meteorological station data and by the outputs from PRECIS nested with ERA-40 and HadAM3P data, respectively. Present day PRECIS simulations possess strong capacity to simulate spatial patterns of present day climate characteristics. However, there also exist some quantitative biases in the HKH region, where PRECIS RCM simulations underestimate temperature and overestimate precipitation with respect to CRU observations. The calibration and validation results of the HBV model experiments show that the performance of HBV-Met is better than the HBV models driven by the PRECIS outputs. However, using input data series from sources different from the data used in the model calibration shows that HBV models driven by the PRECIS outputs are more robust compared to HBV-Met. The Gilgit and Astore river basin, which discharges are depending on the preceding winter precipitation, have higher uncertainties compared to the Hunza river basin which discharge is driven by the energy inputs. The smaller uncertainties in the Hunza river basin may be because of the stable behavior of the input temperature series compared to the precipitation series. The resulting robustness and uncertainty ranges of the HBV models suggest that in data sparse regions such as the HKH region data from regional climate models may be used as input in hydrological models for climate scenarios studies.

1 Introduction

Pakistan's economy is agro-based and highly dependent on the large scale Indus irrigation system. Most of the flow of the river Indus and its tributaries originates from the Hindukush-Karakorum-Himalaya (HKH) region (SIHP, 1990). Impacts of climate change and climate variability on the water resources are likely to affect irrigated agriculture and installed power capacity. Changes in flow magnitudes are likely to raise tensions among provinces, in particular with the downstream areas (Sindh province), with regard to reduced water flows in the dry season and higher flows and resulting flood problems during the wet season. Therefore, modeling the hydrological regime of the HKH region is critical for current and future water resources estimation, planning and operation in Pakistan.

To drive a hydrological model reliable information on local and regional climatological variables (e.g. temperature, precipitation, evapotranspiration, etc.) and their distribution in space and time is required. In many cases, the necessary information can be derived from observational data sets. For large scale hydrological applications and to investigate the impact of climate change on future water resources a hydrological model can be driven with the output from a general circulation model (GCM) (Watson et al., 1996). However, the spatial resolution of GCMs (about 250 km) might be too coarse for hydrological modeling at the basin scale. One way to bridge this scale gap is through statistical downscaling (e.g. Wilby et al., 1999) and an alternative approach is through dynamical downscaling (e.g. Hay et al., 2002; Hay and Clark, 2003). In dynamical downscaling, a regional climate model (RCM) uses GCM output as initial and lateral boundary conditions over a region of interest. The high horizontal resolution of a RCM (about 10–50 km) is more appropriate for resolving the small-scale features of topography and land use, that have a major influence on climatological variables such as precipitation in the climate models. Moreover, the high resolution of the RCM is ideal to capture the spatial variability of precipitation as input to hydrological models (Gutowski et al., 2003). If the resolution of the RCM is not fine enough the bias of the modeled precipitation may lead to an unrealistic hydrological simulation.

Hydrological simulation in data sparse regions as the HKH region using RCM output as input involves a number of problems, including uncertainties in inputs, model parameters and model structure. The most important contribution to the input uncertainty comes from the GCM with additional uncertainties linked to the local scale patterns in downscaling of temperature, precipitation and evapotranspiration in a specific drainage basin (Bergström et al., 2001; Guo et al., 2002). Uncertainties in RCMs for specific parameters can be evaluated and quantified through ensemble simulation (Murphy et al., 2004; Giorgi and Francisco, 2000). Herein, a multitude of model runs is carried out under standardized conditions using either different models or using the same model but with different parameterization schemes, boundary conditions, initializations, resolutions etc.

In many hydrological studies statistical downscaling (Bergström et al., 2001; Pilling and Jones, 2002; Guo et al., 2002; Arnell, 2003; Booij, 2005) and dynamical downscaling (Fowler and Kilsby, 2007; Leander and Buishand, 2007; Bell et al., 2007; Graham et al., 2007) of different GCMs have been used to translate the assumed climate change into hydrological response. However, RCMs could also be used for generating time series of precipitation that are consistent across the region of the RCM. Kay et al. (2006) demonstrated the feasibility of the direct use of RCM data for flood frequency estimation. The results showed that the RCM has a relatively good ability to reproduce flood frequency curves as compared to the flood frequency curves estimated using observed input data. In recent studies, outputs from RCMs have been used in hydrological models by firstly applying a bias correction to RCM simulated precipitation and temperature series (Fowler and Kilsby, 2007; Leander and Buishand, 2007; Bell et al., 2007; Graham et al., 2007).

The aim of this study is to examine the effect of precipitation and temperature simulated with the PRECIS RCM nested in different global data sets on discharge simulated with the HBV model for three river basins in the HKH region. The study area is described in Sect. 2. The HBV climatological inputs and the hydrological model are described in Sect. 3. The results of the PRECIS RCM simulations and calibration and validation results of HBV models are presented in Sect. 4. Finally, the conclusions and recommendations are given in Sect. 5.

2 Description of study area

Three river basins are selected for analysis: Hunza river basin, Gilgit river basin and Astore river basin. The observed discharge data for these three river basins are available at the outlets of the basins. The length of the records in the three river basins is not the same and there are some missing years in the discharge data. Therefore, in some cases the calibration and validation periods in the three river basins are not same. Table 1 lists some features of the study basins and Fig. 1 shows the location of the three river basins. These three river basins are situated in the high mountainous HKH region with many peaks exceeding 7000 m and contain a large area of perennial snow and ice. The surface hydrology of these three river basins is dominated by snow and glacial melt. Climatic variables are strongly influenced by altitude. The HKH region receives a total annual rainfall amount of between 200 and 500 mm, but these amounts are derived from valley-based stations and not representative for elevated zones. High-altitude precipitation estimates derived from accumulation pits runoff above 4000 m range from 1000 mm to more than 3000 mm. These estimates depend on the site and time of investigation, as well as on the method applied (Winger et. al., 2005).

HESSD
5, 865–902, 2008

3 Methodology

3.1 Climatological input

3.1.1 Observed data

Daily observed meteorological data from the Gilgit and Astore meteorological stations are selected for the Gilgit and Astore river basins. There is no meteorological station in the Hunza river basin, therefore neighboring Skardu meteorological station is used for calibration and validation of HBV. The meteorological station data are available for the period 1981–2002. The simulated PRECIS RCM precipitation and temperature data are compared with CRU observations (Mitchell and Jones, 2005) on a monthly basis. This data set is a 0.5° latitude/longitude gridded dataset of monthly terrestrial surface climate for the period 1901–2002.

3.1.2 Regional Climate Model outputs

The RCM used in this study is PRECIS (Providing REgional Climate for Impact Studies) developed by the Hadley Centre of the UK Meteorological Office. The PRECIS RCM is based on the atmospheric component of the HadCM3 climate model (Gordon et al., 2000) and is extensively described in Jones et al. (2004). The atmospheric dynamics module of PRECIS is a hydrostatic version of the full primitive equations and uses a regular longitude-latitude grid in the horizontal and a hybrid vertical coordinate. For this study, the PRECIS model domain for South Asia has been set up with a horizontal resolution of 50×50 km. Some recent studies also have used RCM output at 50×50 km resolution in hydrological studies (e.g. Graham et al., 2007, De Wit et al., 2007). Our domain roughly stretches over latitudes 12.5 to 40.5° N and longitudes 55.5 to 96.5° E. This domain covers India, Pakistan, Afghanistan, the Tibetan Plateau and the HKH region. This domain allows full development of internal mesoscale circulation (e.g. monsoon circulation) and includes relevant regional forcings.

The representation of topography is an important feature of climate models as it has a strong impact on the simulated climate fields, in particular spatial precipitation distribution. Where terrain is flat for thousands of kilometers and away from coasts, the coarse resolution of a GCM may not matter. However, the HKH region has complex orographic features and several mountains exceed 7000 m. Figure 2 shows the topography of the HadAM3P GCM, PRECIS RCM, GTOPO30 2MIN Digital Elevation Model (DEM) and the difference of representation of topography in the driving GCM and PRECIS RCM. The topography of PRECIS RCM (Fig. 2b) is very similar to the topography of GTOPO30 2MIN DEM (Fig. 2c). The difference of representation of topography in the driving GCM and PRECIS RCM (Fig. 2d) clearly shows that the higher resolution of PRECIS RCM provides much better topographic details over the HKH region.

Two global data sets are used to drive the PRECIS model: data from the ERA-40 reanalysis project and the HadAM3P GCM. The horizontal resolution of HadAM3P boundary data is 150 km and for the present climate, it covers the period 1960–1990 (Wilson, 2005). ERA-40 is a re-analysis of meteorological observations produced by the European Centre for Medium-Range Weather Forecasts (ECMWF). It covers the period 1957–2002, has a horizontal resolution of 1.875 by 1.25 degrees (∼187.5 by 125 km) and is extensively described in Uppala et al. (2005).

The PRECIS RCMs driven by HadAM3P and ERA-40 reanalysis boundary data are hereafter referred to as PRECIS Had and PRECIS ERA, respectively. The time periods for PRECIS ERA and PRECIS Had are 1975–2001 and 1960–1990, respectively. The first year in each PRECIS experiment is considered as a spin-up period and these data are not used in any analysis. After post processing of each experiment the time series of temperature and precipitation for three river basins are generated. The PRECIS RCM simulated temperature and precipitation have biases as discussed in Sect. 4.2. These biases are corrected before applying the temperature and precipitation series as input to HBV. For the bias correction a simple bias correction approach as used by Durman et al. (2001) is applied. In this approach a monthly factor based on the ratio of present day simulated values to CRU observed values on a grid box basis is applied to the modelled climatic variables. Recently, Fowler et al. (2007) also used this approach to study the impact of climate change on the water resources in north-west England.

3.2 HBV hydrological model

For the river discharge simulation, the hydrological model HBV of the Swedish Meteorological and Hydrological Institute (SMHI) is used (Bergström, 1995; Lindström et al., 1997). Using inputs from RCMs this model can reproduce the discharge fairly well, e.g. for the river Suir in Ireland (Wang et. al., 2006). It has been widely used in Europe and other parts of the world in e.g. climate change impact studies (Liden and Harlin, 2000; Bergström et al., 2001; Menzel and Bürger, 2002; Booij, 2005, Menzel et. al., 2006). In a recent study, Te Linde et al. (2007) compared the performances of two rainfall-runoff models (HBV and VIC) using different atmospheric forcing data sets and recommended the HBV model for climate change scenarios studies. HBV is a semi-distributed, conceptual hydrological model using sub-basins as the primary hydrological units. It takes into account area-elevation distribution and basic land use categories (glaciers, forest, open areas and lakes). Sub-basins are considered in geographically or climatologically heterogeneous basins. The model consists of six routines, which are a precipitation routine representing rainfall and snow, a soil moisture routine determining actual evapotranspiration and controlling runoff formation, a quick runoff routine and a base flow routine which together transform excess water from the soil moisture routine to local runoff, a transformation function and a routing routine (see Fig. 3).

The precipitation accounting routine defines actual precipitation (P) as rainfall (RF) or snowfall (SF) by application of a threshold value (TT) shown in Eqs. (1) and (2), respectively.

$$RF = pcorr.rfcf.P \qquad T > TT \tag{1}$$

$$SF = pcorr.sfcf.P \qquad T < TT \tag{2}$$

where (T) is actual temperature, *rfcf* is a rainfall correction factor, *sfcf* is a snowfall correction factor and *pcorr* is a general precipitation correction factor. In this routine snowmelt (Sm) is based on a simple degree-day relation given in Eq. (3). The snow pack is assumed to retain melt water as long as the amount does not exceed a certain fraction of the snow. When temperature decreases below TT melt water refreeze (Rmw) according to Eq. (4).

$$Sm = cfmax(T - TT) \tag{3}$$

$$Rmw = cfr.cfmax\,(TT - T) \tag{4}$$

where $cfmax$ is a melting factor and cfr a refreezing factor.

Glacier melting (Gm) will occur only in glacier zones and is taken into account by Eq. (5).

$$Gm = gmelt(T - TT) \tag{5}$$

where $gmelt$ is a glacier melting factor.

The soil moisture routine is the main part controlling runoff formation in which direct runoff, indirect runoff and actual evapotranspiration are generated. Direct runoff occurs if the soil moisture volume (SM) in the catchment, conceptualised through a soil moisture reservoir representing the unsaturated soil, exceeds the maximum soil moisture storage denoted by parameter FC. Otherwise, precipitation infiltrates in the soil moisture reservoir. This infiltrating precipitation (IN) either replenishes the soil moisture content, seeps through the soil layer (R) or evapotranspirates. The indirect runoff (R) through the soil layer is determined by the amount of infiltrating water and the soil moisture content through a power relationship with parameter $BETA$, which is shown in Eq. (6).

$$R = IN\left(\frac{SM}{FC}\right)^{BETA} \tag{6}$$

This indicates that indirect runoff increases with increasing soil moisture content and that when zero infiltration occurs, indirect runoff also becomes zero. Actual evapotranspiration (E_a) depends on the measured potential evapotranspiration (E_p), the soil moisture content and parameter *LP* which is a limit where above the evapotranspiration reaches its potential value. This is shown in Eqs. (7) and (8).

$$E_a = \frac{SM}{LP \cdot FC} \cdot E_p \quad SM < (LP \cdot FC) \tag{7}$$

$$E_a = E_p \qquad SM \geq (LP \cdot FC) \tag{8}$$

At the quick runoff routine three components are distinguished which are percolation to the base flow reservoir, capillary transport to the soil moisture reservoir and quick runoff. Percolation is denoted through parameter *PERC* which is a constant percolation rate, occurring when water is available in the quick runoff reservoir. Capillary transport is a function of the maximum soil moisture storage, the soil moisture content and a maximum value for capillary flow (*CFLUX*) as shown in Eq. (9). If the yield from the soil moisture routine is higher than the percolation and the capillary flow allows, the water becomes available in the quick runoff reservoir for quick flow which is shown by Eq. (10).

$$C_f = CFLUX \cdot \left(\frac{FC - SM}{FC}\right) \tag{9}$$

$$Q_0 = K_f \cdot UZ^{(1+ALFA)}, \tag{10}$$

where *UZ* is the storage in the quick runoff reservoir, *ALFA* a measure for the non-linearity of the flow in the quick runoff reservoir and K_f a recession coefficient.

The slow flow of the catchment is generated in the base flow routine through Eq. (11).

$$Q_1 = K_s \cdot LZ, \tag{11}$$

where *LZ* is the storage in the base flow reservoir and K_s a recession coefficient.

In the transformation routine, the discharge of each sub-catchment is routed through a triangular distribution function and in the routing routine the discharges from the sub-catchments are linked.

In order to assess the performance of the model in simulating observed discharge behaviour an objective function Y is used, which combines the Nash-Sutcliffe efficiency coefficient NS (Nash and Sutcliffe, 1970) and the relative volume error RE and is defined as

$$Y = \frac{NS}{1 + |RE|} \tag{12}$$

where

$$NS = 1 - \frac{\sum_{i=1}^{i=N} [Q_s(i) - Q_o(i)]^2}{\sum_{i=1}^{i=N} \left[Q_o(i) - \overline{Q_o}\right]^2} \tag{13}$$

$$RE = 100 \frac{\sum_{i=1}^{i=N} [Q_s(i) - Q_o(i)]}{\sum_{i=1}^{i=N} Q_o(i)} \tag{14}$$

where i is the time step, N is the total number of time steps, Q_s represents simulated discharge, Q_o is observed discharge and $\overline{Q_o}$ is the mean of Q_o over the calibration or validation period. For a favorable model performance, the efficiency NS should be close to 1 and the RE value should be close to zero resulting in a Y value close to 1.

Depending on the source of input data, i.e. meteorological stations data, PRECIS ERA and PRECIS Had, three HBV models are developed hereafter referred to as HBV-Met, HBV-ERA and HBV-Had, respectively. The first step in the calibration of the HBV models is the selection of parameters. The parameters are selected on the basis of physical reasoning, previous studies and univariate sensitivity analyses. For the three river basins, parameters *gmelt, FC, TT, DTTM* (value added to *TT* to give the threshold temperature for snowmelt), *PERC*, and *cfmax* found to be most sensitive and are selected for calibration. There is a strong interdependence among subsets of these parameters. Therefore in the second step, a multivariate sensitivity analysis is performed to estimate these most sensitive parameters of HBV-Met, HBV-ERA and HBV-Had models for each river basin. For the remaining parameters default values as described in SMHI (2005) are used.

4 Results and discussion

4.1 Spatial patterns of observed and simulated present day climate for South Asia

Figure 4 shows that HadAM3P, PRECIS Had and PRECIS ERA capture the basic spatial patterns of CRU climatology reasonably well. Compared to the CRU observations the simulated PRECIS Had and PRECIS ERA temperature is relatively low in the Tibetan Plateau and in the HKH region. The sharply rising escarpment over the Tibetan Plateau and HKH region results in cooler mountain areas in the PRECIS simulations. In many of these areas, the differences in temperature are due to the higher resolution of topography in PRECIS RCM as compared to the driving GCM.

The spatial patterns of annual mean precipitation as simulated by HadAM3P, PRECIS Had, PRECIS ERA and CRU observations are shown in Fig. 5. The precipitation is maximum over Western Ghats, Eastern Ghats and over the HKH region. The PRECIS RCM simulated precipitation pattern in the present day simulations is quite similar to the CRU observations, indicating that the PRECIS RCM simulations provide an adequate representation of present day conditions. However, some quantitative biases in the spatial patterns exist. In both PRECIS Had and PRECIS ERA wet biases are present over the HKH region. Since the biases are present in both PRECIS Had and PRECIS ERA, some of these biases may be due to errors in the internal model physics of PRECIS RCM and may be related to the inadequate representation of land surface. The model currently uses vegetation distribution and soil properties based on the cli-

HESSD
5, 865–902, 2008

matology of Wilson and Henderson-Sellers (1985). However, this data set does not vary temporally, and seasonal variations in surface albedo, roughness and leaf area index could have a significant effect on the climate (Hudson and Jones, 2002).

4.2 Temporal patterns of observed and simulated present day climate over selected river basins

4.2.1 Temperature

For three river basins, the mean annual cycles of temperature from CRU observations and PRECIS RCM simulations are shown in Fig. 6. The CRU observations show that a mean annual cycle is present in all river basins. The highest mean temperature is reached in July while the lowest mean temperature is observed in January. The influence of height is observed in CRU observations i.e. the highest mean temperature is observed in the lowest river basin (Astore) while the lowest mean temperature is observed in the highest river basin (Hunza). Generally, in all river basins the characteristics of the mean annual cycle of temperature in PRECIS RCM simulations are similar to CRU observations, i.e. the highest mean temperature is observed in July and the lowest in January. This is a sign indicating the correctness of the representation of basic physical processes in the model. In some months, PRECIS Had and PRECIS ERA simulations have some close agreement with each other. The biases in PRECIS RCMs with respect to CRU observations are presented in Table 2. In all three river basins, PRECIS RCM simulations underestimate mean temperature (as already observed in Sect. 4.1). The cold bias in PRECIS RCM simulations may be because of the deficiencies of the GCM simulations (McGregor, 1997). However, the cold bias observed over mountain regions is a common feature of regional climate simulations over different regions of the world (Giorgi et al., 2004; Solman et al., 2008). Therefore, the PRECIS RCM itself may introduce some of the cold bias. It is also observed that cold biases in the winter half-year (i.e. October to March) are relatively higher than in the summer half-year (i.e. April to September). This may be because of the fact that PRECIS

HESSD

5, 865–902, 2008

Title Page
Abstract Introduction
Conclusions References
Tables Figures
◀◀ ▶▶
◀ ▶
Back Close
Full Screen / Esc
Printer-friendly Version
Interactive Discussion

RCM simulations give excessive precipitation during the winter half-year (Fig. 7), which tends to result in excessively wet soils, which cause high latent heat flux, low sensible heat flux, and as a result surface cooling (Bonan, 1998). The magnitude of the cold bias depends on the driving boundary data, e.g. the cold bias during winter is higher in PRECIS Had simulations while it is somewhat less during summer when compared with PRECIS ERA simulations. This latter phenomenon might occur because of less precipitation during these months in PRECIS Had compared to PRECIS ERA.

4.2.2 Precipitation

For three river basins, the mean annual cycles of precipitation from CRU observations and PRECIS RCM simulations are shown in Fig. 7. Generally, CRU observations show the highest precipitation in March and the lowest precipitation in September in all three river basins. The mean annual cycle of precipitation exhibits a stronger variability than the annual cycle of temperature. Overall, for a particular PRECIS RCM experiment all three-study basins have the same patterns. Generally, all PRECIS RCM simulations overestimate precipitation in all three river basins. They give higher precipitation during the winter half-year (October to March) compared to the summer half-year (April to September). Table 3 presents the biases in precipitation of PRECIS RCM simulations with respect to CRU data. The magnitude of biases in PRECIS Had are somewhat less compared to PRECIS ERA. The wet bias can have different causes. Giorgi and Marinucci (1996) showed that the simulation of precipitation may be sensitive to model resolution regardless of the topographic forcing. In particular, in their experiments precipitation tends to increase at finer resolutions. Greater topographic forcing at higher resolution would then further strengthen this effect. Since the study area has a steep topography, this may lead to excessive accumulated orographic precipitation in RCMs (Giorgi et al., 1994).

4.3 Calibration and validation of HBV model

The results of the multiple sensitivity analyses with three calibrated HBV models for three different data sources are described in this section. Table 4 shows the calibrated HBV parameter values for three river basins with three different input data sets. It shows that most parameter values fall within the limits described in other studies (Uhlenbrook et al.,1999; Krysanova et al., 1999; SMHI, 2005; Booij, 2005). However, the parameter values vary between the three data sources in different river basins. During calibration it is noted that for the investigated river basins in the HKH region the threshold temperature *TT* is the most critical parameter, because generally all PRECIS RCM simulations (Figs. 6 and 7) show that most of the precipitation in the HKH region occurs under freezing conditions

Table 5 presents the efficiency *Y*, Nash-Sutcliffe coefficient *NS* and relative volume error *RE* for the three HBV models during calibration and validation periods for the three river basins. All three HBV models show that during the calibration period the relative volume error is very small which indicates that the average simulated and observed discharge are close to each other. General testing of conceptual models (Rango, 1992) has shown that *NS* values higher than 0.8 are above average for runoff modeling in glaciated catchments. Therefore, *NS* values during calibration are satisfactory for all HBV models and the highest values are achieved by HBV-Met (e.g. $0.67<NS<0.87$). Figure 8 presents the observed and simulated discharge of HBV-Met, HBV-ERA and HBV-Had during the calibration period for Hunza river basin. The figures for the other two river basins during the calibration period and figures for all river basins during the validation period are not given for redundancy. During the calibration period the peak values are generally underestimated and discharge during low flow periods is well simulated by the HBV models. During the calibration period efficiency (*Y*) values and visual inspection of hydrographs show that performance of all HBV models is satisfactory.

During validation the *RE* values show that in most cases all models underestimate discharge in the three river basins. Overall, only one out of nine combinations of river basins and HBV models shows a higher efficiency (Y) in the validation compared to the calibration mainly due to the large volume errors. The values of the performance criteria show that during the validation period overall performance of HBV-Met (e.g. $0.63<Y<0.90$) is somewhat better compared to the overall performance of HBV models driven by PRECIS outputs (e.g. $0.42<Y<0.81$). The efficiency is highest for the Hunza river basin compared to the Gilgit and Astore river basins as already observed during calibration. However, comparison of Y values between different river basins has to be regarded carefully, because this statistical measure is strongly influenced by runoff variability. This may explain the relatively low values for the Astore river basin, where runoff variability is highest due to the small size of the river basin.

4.4 Robustness of HBV models

The robustness of HBV models is tested by calibrating the model with one data source and applying the data from the other two data sources. The Absolute Relative Deviation (ARD) in the efficiency (Y) is quantified by Eq. (15)

$$\mathrm{ARD} = 100 \left| \frac{Y_a - Y_c}{Y_c} \right| \tag{15}$$

where Y_c is the efficiency of the model during calibration and Y_a is the efficiency of the model during the application of a different data source.

The efficiency (Y) and Absolute Relative Deviation (ARD) of the three HBV models using input data series from sources different from the data used in the model calibration are shown in Table 6. The values of the efficiencies during the period 1985–1986 show that overall performance of HBV-Met (e.g. $0.20<Y<0.65$) is somewhat less compared to the models using PRECIS RCM data sources (e.g. $0.31<Y<0.86$). The ARD values indicate that the errors in HBV-Met (e.g. $18<\mathrm{ARD}<70$) are somewhat higher compared to the errors in models using PRECIS data sources (e.g. $6<\mathrm{ARD}<46$). This may be due to the fact that in HBV-Met for each river basin only one meteorological station is used for temperature and precipitation input which introduces too much extreme behavior. This resulted in less robust results of HBV-Met when compared with HBV-ERA and HBV-Had. Moreover the values of ARD in HBV-Had are somewhat less compared to HBV-ERA values. This may be related to the small precipitation biases in PRECIS Had compared to PRECIS ERA. The bias correction approach used only corrects the monthly mean and does not consider corrections in the variability. More sophisticated approaches in bias correction (e.g. Leander and Buishand, 2007) may give different results. All these results indicate that the robustness of HBV models is affected by the input forcing data.

The effect of three different input forcing data series on the simulated discharge of HBV is analyzed by calculating the uncertainty range. The uncertainty range in a HBV model is the difference between the maximum and minimum values of the three simulated discharge series. Figure 9 shows the uncertainty range in the three HBV models by applying inputs from three different data sources for three river basins during the 1986 hydrological year. The uncertainties in the three HBV models show that three forcing data series have a large influence on the simulated discharge. The uncertainty range varies among the three river basins. The uncertainties are somewhat less in the Hunza river basin compared to the Gilgit and Astore river basins. This may be due to the fact that the Hunza river basin is heavily glaciated (34%) and temperature play a major role in the summer discharge, whereas the discharge of less glaciated Gilgit (7%) and Astore (16%) river basins depends on the preceding winter precipitation (Archer, 2003). Since in the three different forcing data sets the temperature series are stable compared to the precipitation series and the bias correction technique applied has a larger impact on the precipitation series compared to the temperature series, this resulted in less uncertainties in the simulated discharge of the Hunza river basin compared to Gilgit and Astore river basins.

5 Conclusions and recommendations

Analysis of present day simulations shows that PRECIS possesses strong capacity to simulate spatial patterns of present climate characteristics. However, there also exist some quantitative biases in the spatial patterns especially in mountain regions, where PRECIS RCM simulations underestimate temperature and overestimate precipitation with respect to CRU observations. The biases are highly influenced by the driving forcing data e.g. in the HKH region the precipitation biases in PRECIS Had are somewhat less compared to the biases in PRECIS ERA. The results of our PRECIS RCM simulations follow the same pattern as observed in other studies in the region using PRECIS (Kumar et al., 2006; Yinlong et al., 2006). In all three river basins the annual seasonal temperature cycle is present in all PRECIS simulations. The annual seasonal cycle of precipitation exhibits a stronger variability than the annual cycle of temperature. Overall, in three river basins the magnitude of temperature biases is somewhat higher in PRECIS Had compared to PRECIS ERA simulation whereas the magnitude of precipitation biases is somewhat less in PRECIS Had compared to PRECIS ERA simulation.

The calibration and validation results of the hydrological model HBV driven by observed data and PRECIS RCM present day simulations show that the HBV model can reproduce the discharge reasonably well. In terms of performance criteria, during the calibration period HBV calibrated with observed station data simulates discharge behaviour somewhat better than HBV calibrated with PRECIS RCM data. During the validation period overall performance of HBV-Met is also somewhat better compared to the overall performance of HBV models driven by PRECIS outputs. All three HBV models overestimate discharge at the end of the melt season and underestimate discharge during the peak flow period. Using the input data series from sources different from the data used in the model calibration shows that HBV models calibrated with PRECIS output generally have higher efficiency (Y) and lower absolute relative deviation (ARD) values compared to the corresponding values of HBV-Met. This indicates that

HBV-Had and HBV-ERA are more robust compared to HBV-Met model. The patterns of uncertainties are similar in the three HBV models. The magnitude of uncertainties is higher in the river basins where discharge is dependent on the preceding winter precipitation (i.e. Gilgit and Astore river basins) compared to the river basin which discharge is driven by energy inputs (i.e. Hunza river basin). This is may be because of the fact that the bias correction technique applied here has a larger impact on the precipitation series compared to the temperature series that resulted in smaller uncertainty in the simulated discharge of the Hunza river basin. In terms of both robustness and uncertainty ranges the HBV models calibrated with PRECIS output performed better compared to HBV-Met. Therefore, it is recommended that in data sparse regions as the HKH region data from regional climate models may be used as input in hydrological models for climate scenarios studies.

Acknowledgements. Part of this study was completed at ICTP, Trieste, Italy, which provided funding for two months fellowship for this work. The Higher Education Commission of Pakistan has also provided financial funding. The authors would like to thank the PRECIS team at Hadley Centre, Met Office, UK, for their comments and suggestions during the PRECIS simulations. The boundary data of different GCMs have been kindly supplied by D. Hein on behalf of Hadley Centre, Met Office, UK. The daily river discharge data have been taken from WAPDA, Pakistan. The authors also thank the HBV support team at SMHI for their useful comments and suggestions during the study.

References

Arnell, N. W.: Relative effects of multi-decadal climatic variability and changes in the mean and variability of climate due to global warming: future streamflow in Britain, J. Hydrol., 270, 195–213, 2003.

Archer, D. R.: Contrasting hydrological regime in Indus Basin, J. Hydrol., 274, 198–210, 2003.

Bell, V. A., Kay, A. L., Jones, R. G., and Moore, R. J.: Development of a high resolution grid based river flow model for use with regional climate model out put, Hydrol. Earth Syst. Sci., 11, 532–549, 2007, http://www.hydrol-earth-syst-sci.net/11/532/2007/.

Bergström, S.: The HBV model, Chapter 13 of Computer models of watershed hydrology, Water Resour. Publications, 443–476, 1995.

Bergström, S., Carlsson, B., Gardelin, M., Lindström, G., Pettersson, A., and Rummukainen, M.: Climate change impacts on the runoff in Sweden-assessments by global climate models, dynamical downscaling and hydrological modelling, Clim. Res., 16, 101–112, 2001.

Bonan, G. B.: The Land Surface Climatology of the NCAR Land Surface Model Coupled to the NCAR Community Climate Model, J. Climate, 11, 1307–1326, 1998.

Booij, M. J.: Impact of climate change on river flooding assessed with different spatial model resolutions, J. Hydrol., 303, 176–198, 2005.

De Wit, M. J. M., Van den Hurk, B., Warmerdam, P. M. M., Torfs, P. J. J. F., Roulin, E., and Van Deursen, W. P. A.: Impact of climate change on low-flows in the river Meuse, Climatic Change, 82, 351–372, 2007.

Durman, C. F., Gregory, J. M., Hassell, D. C., Jones, R. G., and Murphy, J. M.: A comparison of extreme European daily precipitation simulated by a global and a regional climate model for present and future climates, Q. J. Roy. Meteor. Soc., 127, 1005–1015, 2001.

Fowler, H. J. and Kilsby, C. G.: Using regional climate model data to simulate historical and future river flows in northwest England, Climatic Change, 80, 337–367, 2007.

Fowler, H. J., Kilsby, C. G., and Stunell, J.: Modelling the impacts of projected future climate change on water resources in north-west England, Hydrol. Earth Syst. Sci., 11, 1115–1126, 2007, http://www.hydrol-earth-syst-sci.net/11/1115/2007/.

Giorgi, F., Bi, X., and Pal, J. S.: Mean, interannual variability and trends in a regional climate change experiment over Europe, I. Present-day climate (1961–1990), Clim. Dynam., 22, 733–756, 2004.

Giorgi, F. and Francisco, R.: Evaluating Uncertainties in the Prediction of Regional Climate Change, Geophys. Res. Lett., 27, 9, 1295–1298, 2000.

Giorgi, F. and Marinucci, M. R.: An investigation of the sensitivity of simulated precipitation to model resolution and its implications of climate studies, Month. Weather Rev., 124, 148–166, 1996.

Giorgi, F., Brodeur, C. S., and Bates, G. T.: Regional climate change scenarios over the United States produced with a nested regional climate model, J. Climate, 7, 375–399, 1994.

Gordon, C. C., Cooper, C., Senior, C. A., Banks, H., Gregory, J. M., Mitchell, J. F. B., and Wood, R. A.: The simulation of SST, sea ice extents and ocean heat transport in a version of the Hadley centre coupled model without flux adjustment, Clim. Dynam., 16, 147–168, 2000.

Graham, L. P., Andreasson, J., and Carlsson, B.: Assessing climate change impacts on hydrology from an ensemble of regional climate models, model scales and linking methods - a case study on the Lule River basin, Climatic Change, 81, 293–307, 2007.

Guo, S., Wang, J., Xiong, L., Yin, A., and Li, D.: A macro-scale and semi-distributed monthly water balance model to predict climate change impacts in China, J. Hydrol., 268, 1–15, 2002.

Gutowski, W. J., Decker, S. G., Donavon, R. A., Pan, Z., Arritt, R. W., and Takle, E. S.: Temporal-spatial scales of observed and simulated precipitation in central U.S. climate, J. Climate, 16, 3841–3847, 2003.

Hay, L. E., and Clark, M. P.: Use of statistically and dynamically downscaled atmospheric model output for hydrologic simulations in three mountainous basins in the western United States, J. Hydrol., 282, 56–75, 2003.

Hay, L. E., Clark, M. P., Wilby, R. L., Gutowski, W. J., Leavesley, G. H., Pan, Z., Arritt, R. W., and Takle, E. S.: Use of regional climate model output for hydrological simulations, J. Hydrometeorol., 3, 571–590, 2002.

Hudson, D. A. and Jones, R. G.: Regional climate model simulations of present-day and future climates over southern Africa, Technical Note 39, Hadley Centre for Climate Prediction and Research, Met Office, Bracknell, UK, 2002.

Jones, R. G., Noguer, M., Hassell, D. C., Hudson, D., Wilson, S. S., Jenkins, G. J., and Mitchell, J. F. B.: Generating high resolution climate change scenarios using PRECIS, Met Office Hadley Centre, Exeter, UK, 40 pp., 2004.

Kay, A. L., Jones, R. G., and Reynard, N. S.: RCM rainfall for UK flood frequency estimation, I. Method and validation, J. Hydrol., 318, 151–162, 2006.

Krysanova, V., Bronstert, A., and Muller-Wohlfeil, D. I.: Modelling river discharge for large drainage basins: from lumped to distributed approach, Hydrol. Sci. J., 44, 313–331, 1999.

Kumar, R. K., Sahai, A.K., Kumar, K. K., Patwardhan, S. K., Mishra, P.K., Revadekar, J. V., Kamala, K., and Pant, G.B.: High-resolution climate change scenarios for India for the 21st century, Curr. Sci. India, 90, 334–345, 2006.

Leander, R. and Buishand, T. A.: Resampling of regional climate model output for the simulation of extreme river flows, J. Hydrol., 332, 487–496, 2007.

Liden, R. and Harlin, J.: Analysis of conceptual rainfall-runoff modelling performance in different climates, J. Hydrol., 238, 231–247, 2000.
Lindström, G., Johansson, B., Persson, M., Gardelin, M., and Bergström, S.: Development and test of the distributed HBV-96 model, J. Hydrol., 201, 272–288, 1997.
McGregor, J. L.: Regional climate modeling, Meteorol. Atmos. Phys., 63, 105–117, 1997.
Menzel, L., Thieken, A. H., Schwandt, D., and Bürger, G.: Impact of climate change on the regional Hydrology-Scenarios-Based modelling studies in the German Rhine Catchment, Nat. Hazards, 38, 45–61, 2006.
Menzel, L. and Bürger, G.: Climate change scenarios and runoff response in the Mulde catchment (Southern Elbe, Germany), J. Hydrol., 267, 53–64, 2002.
Mitchell, T. D. and Jones, P. D.: An improved method of constructing a database of monthly climate observations and associated high-resolution grids, Int. J. Climatol., 25, 693–712, 2005.
Murphy, J. M., Sexton, D., Barnett, D., Jones, G., Webb, M., Collins, M., and Stainforth, D.: Quantification of modelling uncertainties in a large ensemble of climate change simulations, Nature, 430, 768–772, 2004.
Nash, J. E. and Sutcliffe, J. V.: River flow forecasting through conceptual models 1: a discussion of principles, J. Hydrol., 10, 282–290, 1970.
Pilling, C. G. and Jones, J. A. A.: The impact of future climate change on seasonal discharge, hydrological processes and extreme flows in the Upper Wye experimental catchment, mid-Wales, Hydrol. Process., 16, 1201–1213, 2002.
Rango, A.: Worldwide testing of the snowmelt runoff model with applications for predicting the effects of climate change, Nord. Hydrol., 23, 155–172, 1992.
SMHI.: Integrated hydrological modelling system (IHMS), Manual version 5.6, SMHI, Norrkoping, 2005.
SIHP.: Snow and Ice Hydrology Project, Upper Indus Basin, Overall. Report, WAPDA- IDRC-Wilfrid Laurier University, 179 pp., 1990.
Solman, S. A., Nunez, M. N., and Cabre, M. F.: Regional climate change experiments over southern South America. I: present climate, Clim. Dynam., 30, 533–552, 2008.
Te Linde, A. H., Aerts, J. C. J. H., Hurkmans, R. T. W. L., and Eberle, M.: Comparing model performance of two rainfall-runoff models in the Rhine basin using different atmospheric forcing data sets, Hydrol. Earth Syst. Sci. Discuss., 4, 4325–4360, 2007, http://www.hydrol-earth-syst-sci-discuss.net/4/4325/2007/.

Uhlenbrook, S., Seibert, J., Leibundgut, C., and Rodhe, A.: Prediction uncertainty of conceptual rainfall-runoff models caused by problems in identifying model parameters and structure, Hydrol. Sci. J., 44, 779–797, 1999.
Uppala, S. M., Kållberg, P. W., Simmons, A. J., Andrae, U., Da Costa Bechtold, V., Fiorino, M., Gibson, J. K., Haseler, J., Hernandez, A., Kelly, G. A., Li, X., Onogi, K., Saarinen, S., Sokka, N., Allan, R. P., Andersson, E., Arpe, K., Balmaseda, M. A., Beljaars, A. C. M., Van De Berg, L., Bidlot, J., Bormann, N., Caires, S., Chevallier, F., Dethof, A., Dragosavac, M., Fisher, M., Fuentes, M., Hagemann, S., Holm, E., Hoskins, B. J., Isaksen, L., Janssen, P. A. E. M., Jenne, R., McNally, A. P., Mahfouf, J. F., Morcrette, J. J., Rayner, N. A., Saunders, R. W., Simon, P., Sterl, A., Trenberth, K. E., Untch, A., Vasiljevic, D., Viterbo, P., and Woollen, J.: The ERA-40 re-analysis, Q. J. Roy. Meteor. Soc., 131, 2961–3012, 2005.
Wang, S., McGrath, R., Semmler, T., Sweeney, C., and Nolan, P.: The impact of the climate change on discharge of Suir river catchment (Ireland) under different climate scenarios, Nat. Hazards Earth Syst. Sci., 6, 387–395, 2006, http://www.nat-hazards-earth-syst-sci.net/6/387/2006/.
Watson, R. T., Zinyowera, M. C., and Moss, R. H.: Climate Change 1995: Impacts, Adaptations, and Mitigations of climate change, Cambridge University Press, 889 pp., 1996.
Wilby, R. L., Hay, L. E., and Leavesley, G. H.: A comparison of downscaled and raw GCM output: Implications for climate change scenarios in the San Juan River Basin, Colorado, J. Hydrol., 225, 67–91, 1999.
Wilson, M.F. and Hendersen-Sellers, A.: A global archive of land cover and soils data for use in general circulation models, J. Climatol., 5, 119–143, 1985.
Wilson, S., Hassell, D., Hein, D., Jones, R., and Taylor, R.: Installing and using the Hadley Centre regional climate modelling system, PRECIS (version 1.4), Met Office Hadley Centre, Exeter, UK, 2005.
Winger, M., Gumpert, M., and Yamout, H.: Karakorum-Hindukush-western Himalaya: assessing high-altitude water resources, Hydrol. Process., 19, 2329–2338, 2005.
Yinlong, X., Yong, Z., Erda, L., Wantao, L., Wenjie, D., Jones, R., Hassell, D., and Wilson, S.: Analysis on the climate change responses over China under SRES B2 scenario using PRECIS, Chinese Sci. Bull., 51, 2260–2267, 2006.

Table 1. Characteristics of study area.

	River basin		
	Hunza	Gilgit	Astore
Discharge gauging station	Dainyor	Gilgit	Doyian
Latitude	35°56′	35°56′	35°33′
Longitude	74°23′	74°18′	74°42′
Elevation of gauging station (m)	1450	1430	1583
Drainage area (km^2)	13 925	12 800	3750
Glacier covered area (km^2)	4688	915	612
Mean elevation (m)	4472	3740	3921
% area above 5000 m	35.8	2.9	2.8
No. of meteorological stations			
Precipitation	–	1	1
Temperature	–	1	1
No. of PRECIS grid points	6	5	2

HESSD
5, 865–902, 2008
Use of RCM simulations as input for hydrological models
M. Akhtar et al.

Table 2. Biases in mean temperature (˚C) as simulated with two PRECIS RCMs relative to CRU reference data for different seasons and river basins (JFM=January, February, March, etc.).

Season	PRECIS ERA			PRECIS Had		
	Astore	Gilgit	Hunza	Astore	Gilgit	Hunza
JFM	−2.3	−6.0	−5.5	−7.7	−6.1	−7.5
AMJ	−2.0	−5.2	−6.7	−2.9	−2.0	−4.9
JAS	−0.2	−3.8	−6.5	−1.9	−2.4	−6.0
OND	−3.4	−8.4	−9.1	−8.4	−8.0	−10.3

Table 3. Biases in precipitation (%) as simulated with two PRECIS RCMs relative to CRU reference data for different seasons and river basins (JFM=January, February, March, etc.).

Season	PRECIS ERA			PRECIS Had		
	Astore	Gilgit	Hunza	Astore	Gilgit	Hunza
JFM	263	105	276	61	3	128
AMJ	147	104	279	49	26	125
JAS	34	−42	341	24	−20	371
OND	426	130	334	102	−26	96

HESSD

5, 865–902, 2008

Use of RCM simulations as input for hydrological models

M. Akhtar et al.

Table 4. Parameter values for HBV for three river basins with three different input data sets.

Parameter	HBV-Met			HBV-ERA			HBV-Had		
	Hunza	Gilgit	Astore	Hunza	Gilgit	Astore	Hunza	Gilgit	Astore
cfmax	3	3	4.5	3.2	3	3.5	3	3	3.5
DTTM	0	−2.5	−2.5	−1	−1.5	−1.5	−1.5	−2.5	−2.5
FC	1500	700	700	100	700	700	1100	700	700
gemelt	3.5	4	4.5	3.5	3.5	4	4	3.4	4.5
PERC	0.5	0.8	0.8	0.5	0.5	0.5	0.5	0.9	0.5
TT	0	−2	−2.5	−0.3	−1.5	0	0.4	−2	−1.5

Table 5. Performance of three HBV models during calibration and validation in different river basins.

		Calibration				Validation			
Model	Rive basin	Period	*NS*	*RE* %	*Y*	Period	*NS*	*RE* %	*Y*
HBV-Met	Hunza	1981–1990	0.874	−0.4	0.87	1991–1996	0.910	−1.4	0.90
	Gilgit	1981–1990	0.825	−0.4	0.82	1991–1996	0.770	−11.7	0.69
	Astore	1981–1990	0.677	−1.2	0.67	1991–1996	0.726	−15.2	0.63
HBV-ERA	Hunza	1981–1990	0.891	0	0.89	1991–1996	0.828	1.6	0.81
	Gilgit	1981–1990	0.750	0.2	0.75	1991–1996	0.759	−10.6	0.69
	Astore	1981–1990	0.577	0	0.58	1991–1996	0.515	−22.7	0.42
HBV-Had	Hunza	1981–1990	0.769	0	0.77	1975–1980	0.696	−25.4	0.56
	Gilgit	1981–1990	0.740	0.3	0.74	1965–1970	0.758	−8.8	0.70
	Astore	1981–1990	0.620	−2.3	0.61	1975–1980	0.622	5.0	0.59

HESSD
5, 865–902, 2008

Table 6. Efficiency *Y* of three HBV models using data sources different from the calibration sources during the hydrological years 1985 and 1986 in different river basins. The values of absolute relative deviations (ARD) are given in parentheses. The italic values indicate efficiency *Y* during calibration.

River Basin	Model	Data Source Applied		
		Met Observations	PRECIS ERA	PRECIS Had
Hunza	HBV-Met	*0.87*	0.65(25)	0.53(39)
	HBV-ERA	0.49(45)	*0.89*	0.73(18)
	HBV-Had	0.56(27)	0.86(12)	*0.77*
Gilgit	HBV-Met	*0.82*	0.55(33)	0.62(24)
	HBV-ERA	0.57(24)	*0.75*	0.63(16)
	HBV-Had	0.67(9)	0.64(14)	*0.74*
Astore	HBV-Met	*0.67*	0.20(70)	0.55(18)
	HBV-ERA	0.31(46)	*0.58*	0.37(36)
	HBV-Had	0.57(6)	0.35(43)	*0.61*

HESSD

5, 865–902, 2008

Title Page
Abstract | Introduction
Conclusions | References
Tables | Figures
◀▌ | ▶▌
◀ | ▶
Back | Close
Full Screen / Esc

Printer-friendly Version

Interactive Discussion

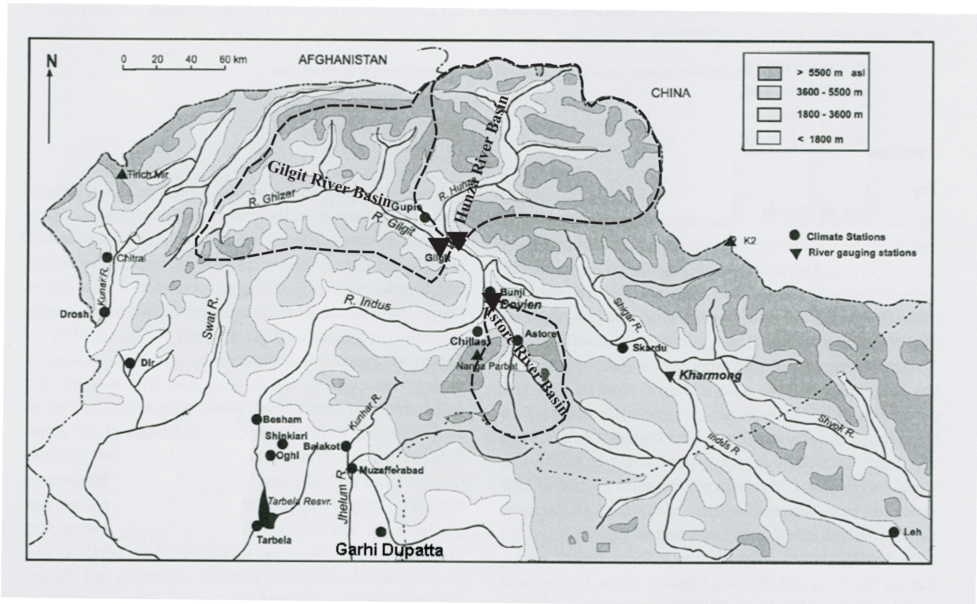

Fig. 1. Location of three river basins.

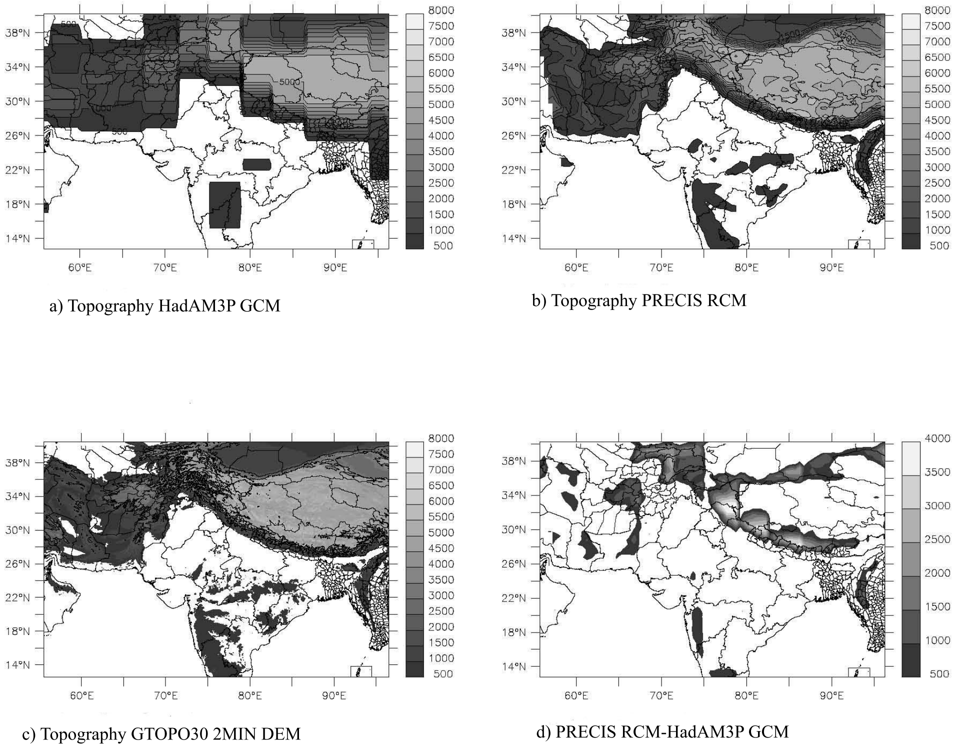

Fig. 2. Topography of selected domain. **(a)** Topography of HadAM3P GCM. **(b)** Topography of PRECIS. **(c)** Topography of the GTOPO30 2MIN DEM **(d)** Deviation of PRECIS RCM topography from GCM topography.

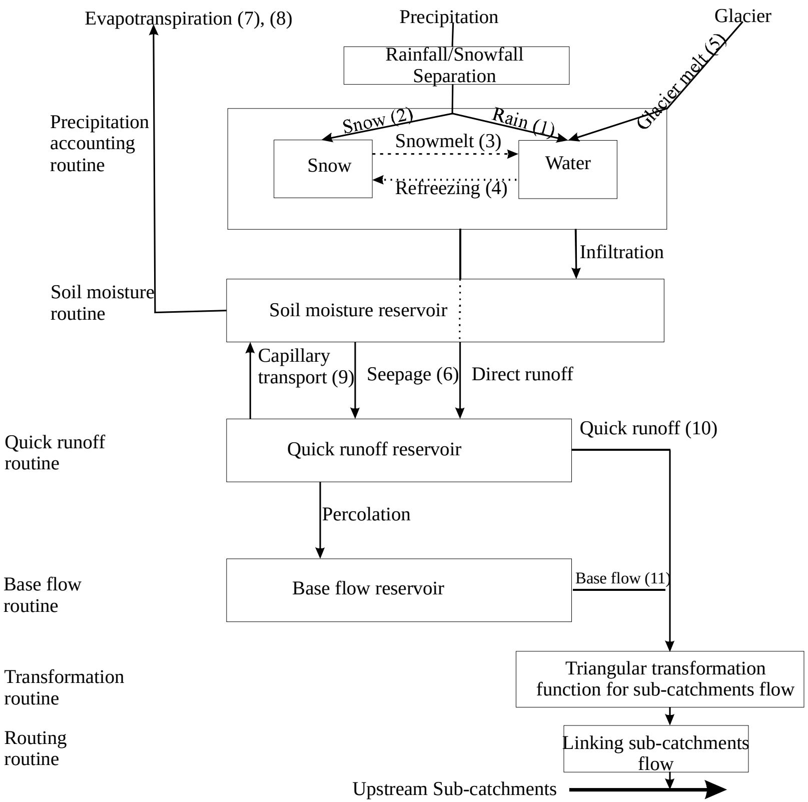

Fig. 3. Schematisation of the hydrological model HBV (based on Lindström et al., 1997); numbers between brackets refer to described equations.

HESSD
5, 865–902, 2008

Use of RCM simulations as input for hydrological models

M. Akhtar et al.

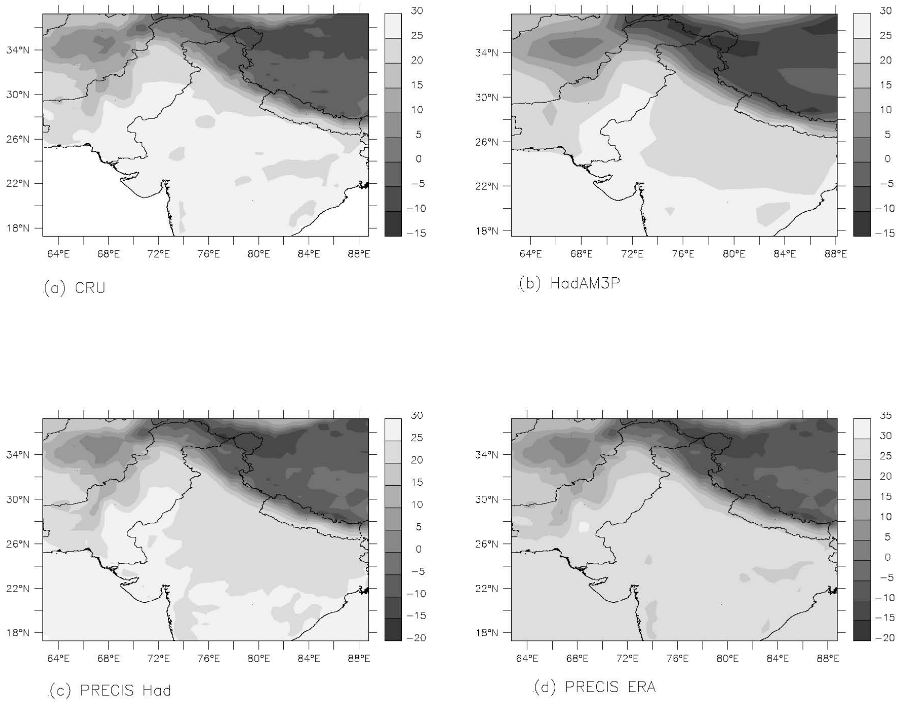

Fig. 4. Observed and simulated present day patterns of annual mean temperature (°C) for **(a)** CRU data, **(b)** GCM HadAM3P, **(c)** PRECIS Had and **(d)** PRECIS ERA.

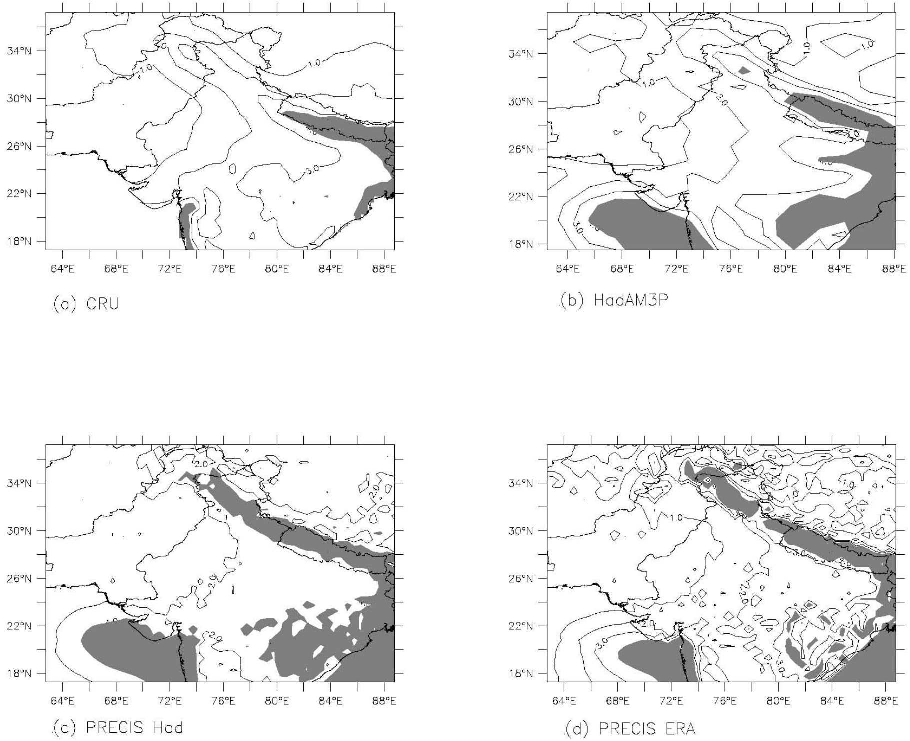

Fig. 5. Observed and simulated present day patterns of annual mean precipitation (mm/d) for **(a)** CRU data, **(b)** GCM HadAM3P, **(c)** PRECIS Had and **(d)** PRECIS ERA. The shaded area indicates precipitation above 4 mm/d in all the panels.

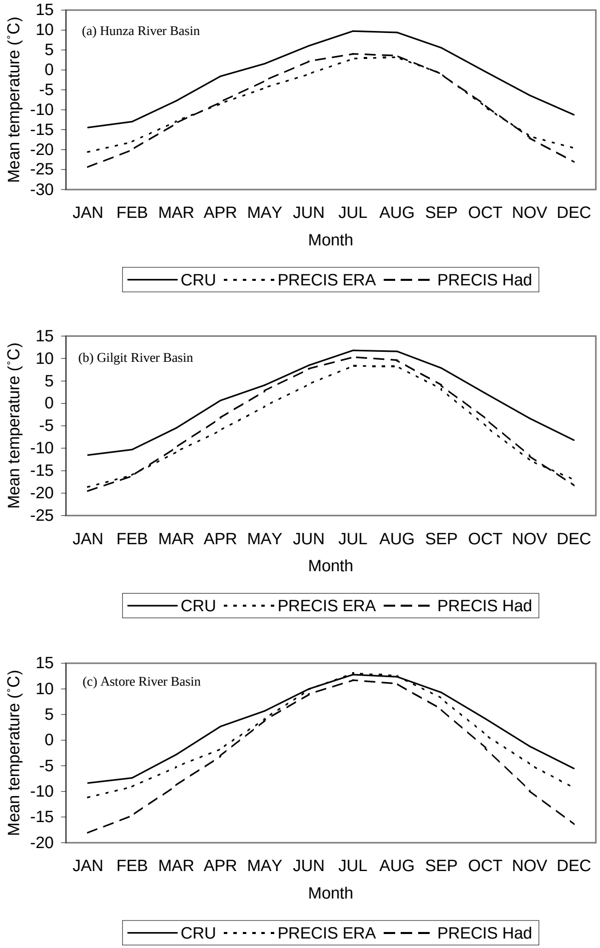

Fig. 6. Mean annual cycle of temperature over **(a)** Hunza river basin **(b)** Gilgit river basin **(c)** Astore river basin as simulated with PRECIS RCMs and from CRU data [°C].

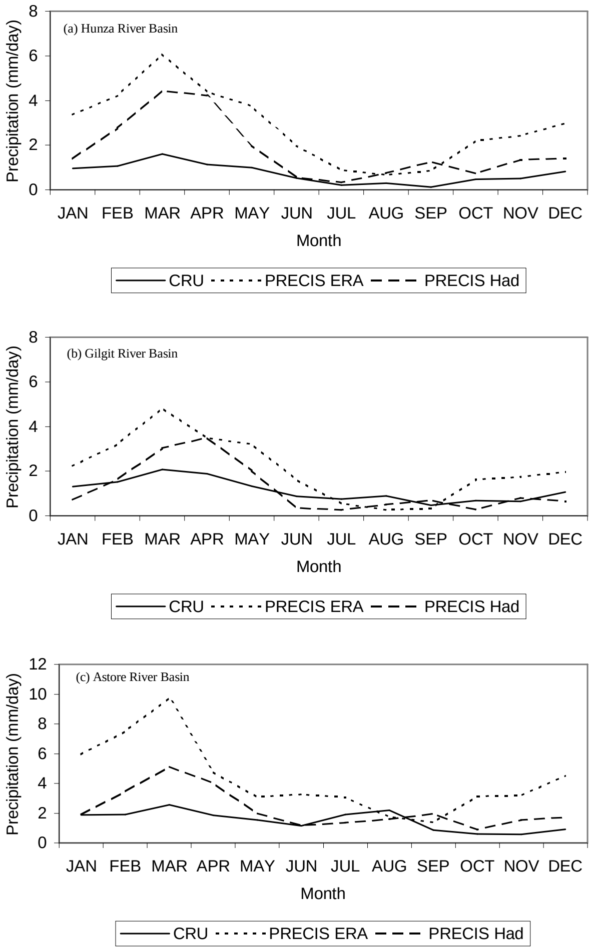

Fig. 7. Mean annual cycle of precipitation over **(a)** Hunza river basin **(b)** Gilgit river basin **(c)** Astore river basin as simulated with PRECIS RCMs and from CRU data [mm/d].

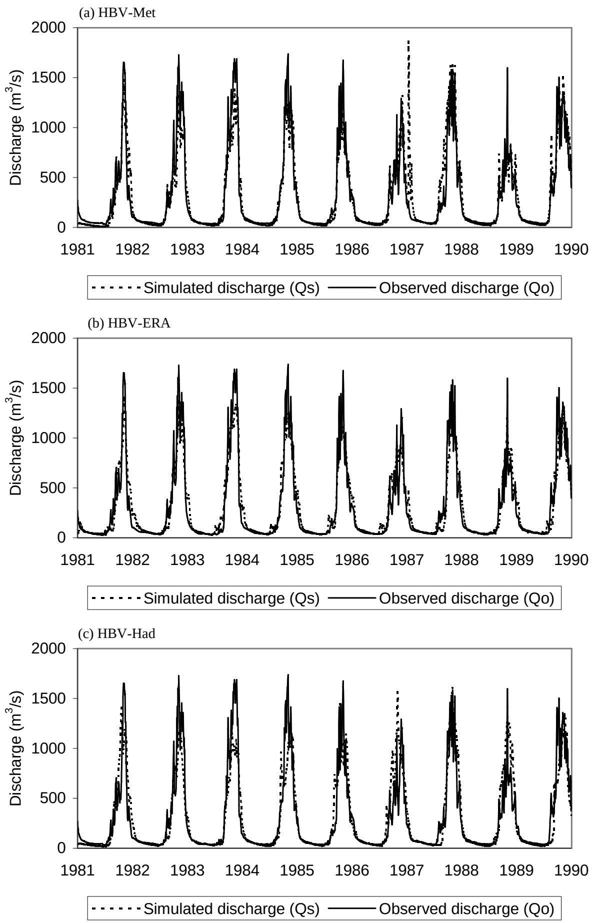

Fig. 8. Observed (Q_o) and simulated (Q_s) discharge (m^3/s) of **(a)** HBV-Met, **(b)** HBV-ERA and **(c)** HBV-Had for the Hunza river basin during calibration period.

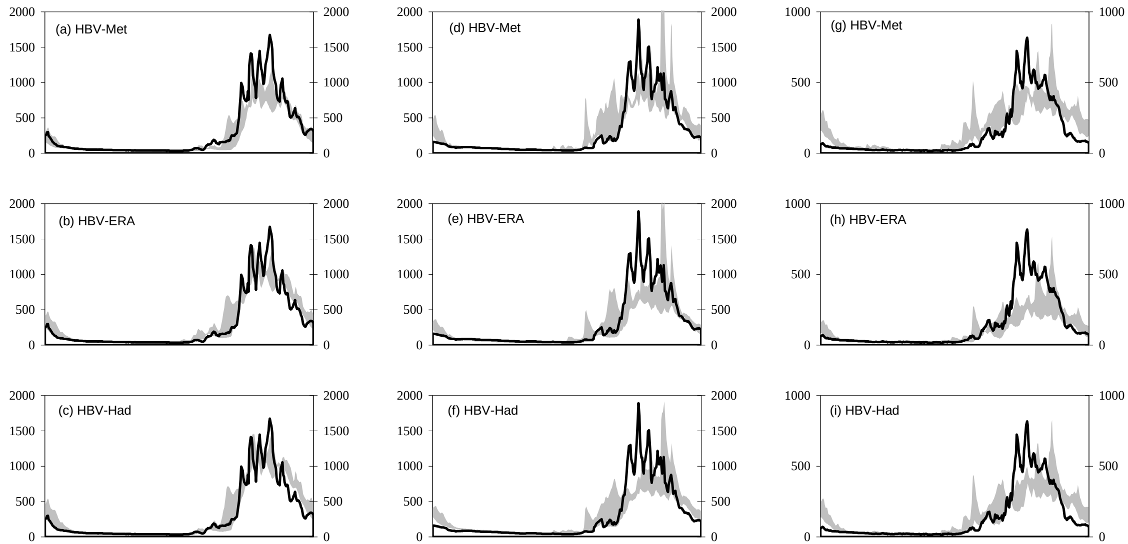

Fig. 9. Observed discharge (black line) and uncertainties (gray shade) in simulated discharge of HBV-Met, HBV-ERA and HBV-Had for **(a–c)** Hunza (left panel), **(d–f)** Gilgit (central panel) and **(g–i)** Astore (right panel) river basins during the 1986 hydrological year.

HESSD
5, 865–902, 2008

Use of RCM simulations as input for hydrological models

M. Akhtar et al.